JOURNAL OF SOLID STATE CHEMISTRY 59, 210–219 (1985)

Vibrational Study of the Unusual Phase Sequence in $Tl_3Cr(SO_4)_3$: A Compound Containing $[Cr(SO_4)_3^{3-}]_\infty$ Columns

CLAUDE BRÉMARD* AND JACKY LAUREYNS

Laboratoire de Spectrochimie Infrarouge et Raman CNRS, Université Sciences et Techniques de Lille I, 59655 Villeneuve d'Ascq Cédex, France

AND FRANCIS ABRAHAM AND GUY NOWOGROCKI

Laboratoire de Cristallochimie et Physicochimie du Solide UA-CNRS 452, Ecole Nationale Supérieure de Chimie de Lille, B.P. 108, 59652 Villeneuve d'Ascq Cédex, France

Received October 12, 1984; in revised form January 9, 1985

The polarized Raman spectra of small single crystals of $Tl_3Cr(SO_4)_3$ have been recorded using the Raman microprobe technique in the temperature range 295–660 K. The behavior of the external modes is analyzed on polycrystalline samples with conventional Raman spectrometer from 100 K to the decompositon temperature 660 K. Analysis of the spectra, in connection with dielectric measurements and X-ray data show that $Tl_3Cr(SO_4)_3$ undergoes the following space group phase sequence

$$P2_1/c \xrightarrow{340\ K} R\bar{3} \xrightarrow{450\ K} R3c \xrightarrow{630\ K} R\bar{3}c$$

in accordance with the point group relationship

$$2/m \rightarrow \bar{3} \rightarrow 3m \rightarrow \bar{3}m.$$

Introduction

Recently, compounds of general formula $M^{I}_3M'^{III}(SO_4)_3$ have attracted attention (*1*) as some of them undergo phase transition of a ferroelastic nature (*2*).

The existence of both unstable intermediate and prototype phases have been postulated (*2*) to explain the transition mechanism between monoclinic and trigonal symmetry. There are no vibrational data available on the columnar compounds $M^{I}_3M'^{III}(SO_4)_3$ to date. In order to get a better understanding of the phase transitions exhibited by these compounds we have undertaken a Raman investigation of the phase transitions in $Tl_3Cr(SO_4)_3$. X-Ray studies, dielectric measurements, and Raman experiments show that the existence of such intermediate and prototype phases is well substantiated.

Experimental

$Tl_3Cr(SO_4)_3$ was prepared as described previously (*3*). The Raman spectra of the powder samples of $Tl_3Cr(SO_4)_3$ were obtained using a DILOR RT 30 instrument equipped for photon counting. The spectra were recorded from 100 to 660 K in the

* To whom correspondence should be addressed.

0022-4596/85 $3.00

right-angle and back-scattering geometries. Sample spinning-cell techniques were used in order to avoid any decomposition and any phase transformation induced by the laser beam. The exciting lines used the 514.5-nm radiation of an argon-ion laser and the 647.1-nm radiation of a krypton-ion laser.

The infrared transmission and reflection spectra were run with a Bruker IFS 113V Fourier-transform spectrometer. The infrared transmission spectra were recorded in the range 4000–20 cm^{-1} at room temperature using pressed KBr disks (4000–400 cm^{-1}) and pressed polyethylene disks (400–20 cm^{-1}). In addition, the polycrystalline material was examined as an emulsion in Nujol between CsI windows. The transmission infrared spectra of phase I or phase II samples are identical at room temperature. The weak pressure between the CsI windows generates the irreversible phase transition phase I → phase II. The diffuse reflectance spectra were recorded in the range 4000–400 cm^{-1} to avoid any phase transformation by this pressure effect.

The single crystals used for Raman studies were kindly provided by Dr. G. Laplace and Dr. B. Jolibois. Unfortunately, the crystals were too small and too sensitive to laser-beam heating for conventional Raman study, so the polarized Raman spectra have been recorded using the Raman microprobe (MOLE) (*4*) equipped for photon counting and accumulation of spectra. The crystals are transparent with a slight green coloration, they are prismatic with hexagonal cross section. A crystal with dimensions 0.015 mm between the lateral faces and 0.096 mm between hexagonal sections was selected for Raman microprobe experiments. The orientation of the crystal was determined by X rays. Figure 1 shows the experimental arrangement for the polarized Raman scattering. The polarized Raman spectra were recorded from 295 to 660 K using low power, 2 mW at sample, of the

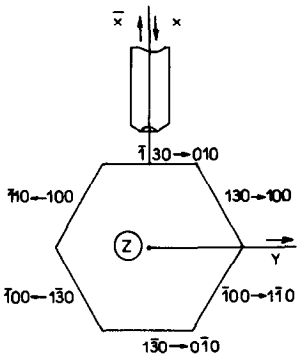

FIG. 1. Raman scattering geometry in the microprobe experiment. The crystal faces ($P2_1/c$ and $R\bar{3}$) are shown. The C axis is parallel to Z.

488.0- and 514.5-nm laser lines. The configuration of the laser Raman molecular microprobe (MOLE) has been previously described (*4*). The same objective of a conventional optical microscope is used to focus the laser beam into a spot on the part of the sample to be analyzed and to collect the scattered light at the focal point. The incident laser beam was passed through a polarization rotator to obtain the different polarization geometries and the scattered light was analyzed by a polaroid plate and passed through a compensated quartz wedge scrambler before entering the slit of the optical filter. The effects of the beam splitter must be compensated (*5*) to perform such measurements with the MOLE. In addition, the quartz wedge polarization scrambler may not be completely effective in scrambling the plane polarized light emerging from the analyzer.

Both of these effects can be determined by passing white depolarized light through the optical path and measuring the signal as a function of frequency for the two positions of the analyzer. Although the optical geometry used in Raman microspectroscopy is very different from the conventional one, polarization measurements can be made. Even with the very wide aperture objectives that are usually employed, polarization "leakage" is not large (*6*): less than

TABLE I

CORRELATIONS FOR SO_4^{2-} IONS IN PHASE I

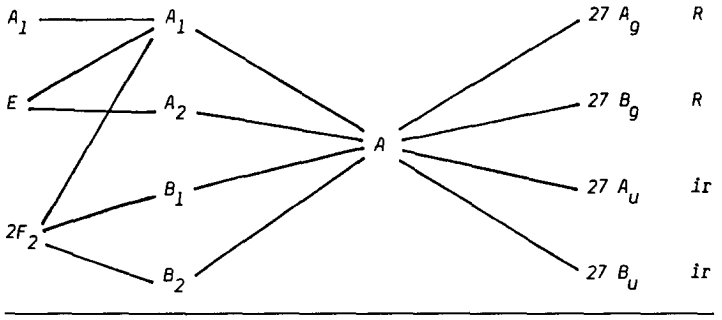

3%. The spectra obtained at several spots of all the six lateral faces of the crystal are identical with the same polarization conditions. These results point out the homogeneity of the crystal.

Analysis of the Normal Modes

Group theoretical analysis was carried out and a vibrational assignment was proposed on the basis of the C_{2h}^5, C_{3i}^2, and C_{3v}^6 symmetries.

By analogy with $(NH_4)_3In(SO_4)_3$ (*1*), we assumed that phase I of $Tl_3Cr(SO_4)_3$ belongs to the monoclinic space group $P2_1/c \equiv C_{2h}^5$, with four formula units per unit cell. Each atom is located on sites of C_1 symmetry. A factor-group analysis yields $57A_g + 57B_g + 56A_u + 55B_u$ optic modes. The A_g and B_g modes are only Raman active, the A_u and B_u modes are infrared active. The three acoustic modes correspond to translational lattice motions $A_u + 2B_u$. See Table I.

—In phase II of $Tl_3Cr(SO_4)_3$ [$R\bar{3} \equiv C_{3i}^2$], the primitive cell is rhombohedral and contains two formula units (*7*). The Cr atoms occupy *a* and *b* sites of C_{3i} symmetry, the O, S, and Tl atoms are on *f* sites of C_1 symmetry. This

TABLE II

CORRELATIONS FOR SO_4^{2-} IONS IN PHASE II

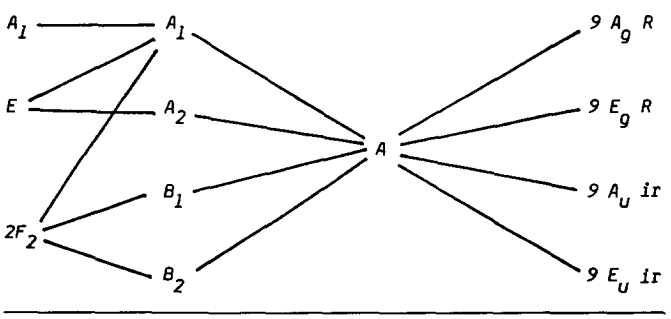

TABLE III

CORRELATIONS FOR SO_4^{2-} IONS IN PHASE III

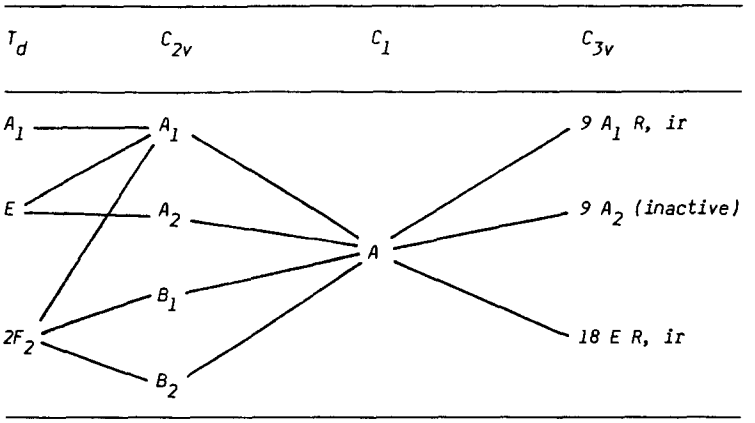

configuration predicts $18A_g + 18E_g$ Raman modes, $19A_u + 19E_u$ infrared modes and $A + E_u$ acoustic modes. See Table II.

—In phase III of $Tl_3Cr(SO_4)_3$ [$R3c \equiv C_{3v}^6$, $Z = 2$] (*7*) the two Cr atoms occupy a site of C_3 symmetry, the O, S, and Tl atoms are on six sites of C_1 symmetry. The $18A_1 + 37E$ vibrations become infrared and Raman active, the $19A_2$ species are optically inactive. The acoustic modes are $A_1 + E$. See Table III.

Results and Discussion

Monoclinic phase $P2_1/C \equiv C_{2h}^5$

Stuctural determinations performed on the two phases of $(NH_4)_3In(SO_4)_3$ show a one-dimensional arrangement (*1*, *2*). In $M_3^IM'^{III}(SO_4)_3$, building blocks of the structure are $M'^{III}O_6$ octahedra and SO_4 tetrahedra, linked together to form infinite columns $[M'^{III}(SO_4)^{3-}]_\infty$ (Fig. 2) along the $\vec{c}$ axis of the monoclinic or hexagonal cell; the M^I ions connect these chains by electrostatic interactions.

Some of the expected Raman active modes were observed at 300 K for the phase I of $Tl_3Cr(SO_4)_3$ in the powder spectra. It should be noted that the cooling of the product to 100 K does not generate further siginificant splitting of the Raman bands. Using powders, uncompletely resolved Raman spectra (Fig. 3) as well as diffuse reflectance infrared spectra are obtained. An attempt to separate these different modes into internal and external vibrations has been made. Indeed, the widths of the Raman bands are quite different. The bands at lower frequencies, less than 70 cm^{-1}, hardly change with temperature from

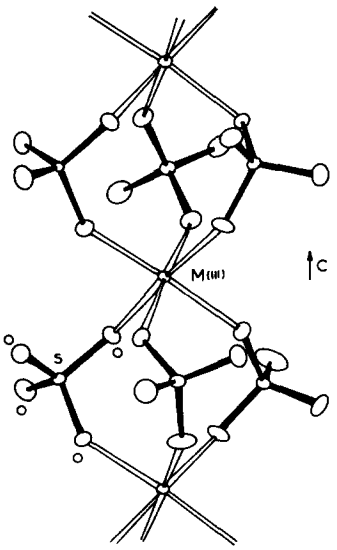

FIG. 2. Structure of inifinite columns of $[In(SO_4)_3^{3-}]_\infty$ in $(NH_4)_3In(SO_4)_3$ from Ref. (*1*).

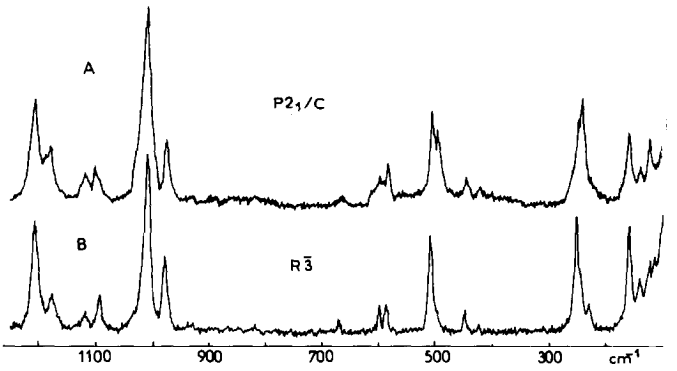

FIG. 3. Unpolarized Raman spectra of $P2_1/c$ powder samples and $R\bar{3}$ phases of $Tl_3Cr(SO_4)_3$.

100 to 340 K in frequency or in line width: this suggests that they have mostly translational character (*8–10*). The low-lying phonons detected below 70 cm^{-1} (Fig. 4) are assigned to translational modes of Tl^+ against rigid $[Cr(SO_4)_3^{3-}]_\infty$ chains (*10*). The remaining bands are due to the vibrations of the molecules in the chains. The separation between A_g and B_g modes can be experimentally made if the Raman spectra are recorded under polarization conditions. With the small crystal used, only four polarized spectra could be obtained: $X(YY)\bar{X}$, $X(ZZ)\bar{X}$, and $X(YZ)\bar{X}$.

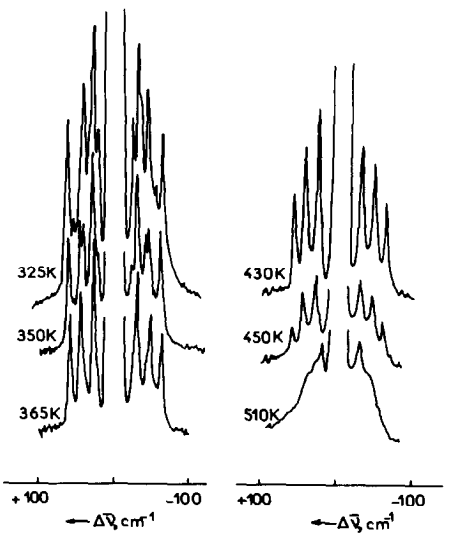

FIG. 4. Low-frequency Raman spectra of powder samples of $Tl_3Cr(SO_4)_3$ at several temperatures. Excitation 514.5 nm.

The highest frequency modes are due to skeletal stretching vibrations of the SO_4 groups—$11A_g$ and $11B_g$ modes were found in the range 1300–900 cm^{-1} in the polarized Raman spectra (Figs. 5A and B, and Table IV). The spectra may be compared to those of H_2SO_4 (*8*), $KHSO_4$ (*9*), and $RbHSO_4$ (*10*) crystals. The bridging of the chromium atoms by the SO_4^{2-} ions lengthens the two S—O distances and shortens the free S=O bonds. In a first approximation the SO_4 groups can be considered as tetrahedral, T_d, and in a second approximation of C_{2v} symmetry. In consequence the triply degenerate F_2 mode of SO_4^{2-} ion would split into $A_1 + B_1 + B_2$ modes. This effect is clearly observed in the Raman (Fig. 3) and diffuse reflectance infrared spectra (Fig. 7) obtained with powder samples. The separations between A_g and B_g Raman bands and A_u and B_u infrared bands are not large, and are poorly resolved in the unpolarized spectra.

The static and dynamic fields produce further splitting into a number corresponding to the expected $12A_g + 12B_g$ Raman bands in the range 1300–900 cm^{-1}. The higher frequencies are assigned to the stretching of the shortest S—O bonds of the SO_4 groups and the lower frequencies

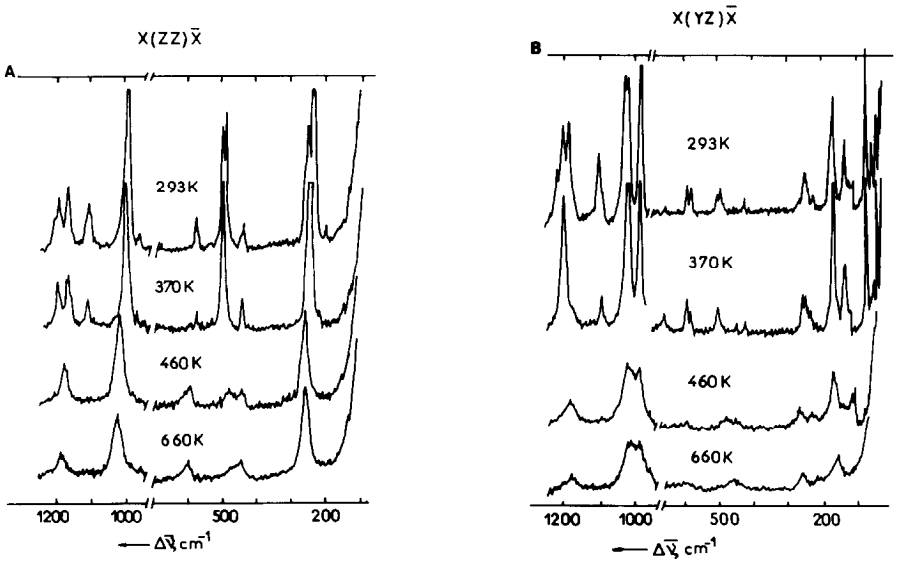

FIG. 5. Polarized Raman spectra in $X(ZZ)\bar{X}$ (A) and $X(YZ)\bar{X}$ (B) orientation of the different phases of $Tl_3Cr(SO_4)_3$ at several temperatures. Excitation 541.5 nm.

are associated to the stretching of the S—O bonds in the Cr—O—S—O—Cr bridge (*11*).

There are two groups of bands in the regions 680–580 and 450–420 cm^{-1} due to skeletal bending modes and they can be compared to those of other sulfate compounds (*8–11*). However, the deformation modes of the SO_4 groups are probably coupled with the internal modes of the distorted CrO_6 octahedra and a straightforward assignment cannot be obtained.

The strong A_g bands at 496, 506 and 259, 242 cm^{-1} can be assigned to Cr—O modes (*12*) in CrO_6 moieties in accordance with the relative intensities of the Raman bands corresponding to stretching, bending vibrations of SO_4 groups and skeletal modes of CrO_6. No attempt was undertaken to assign the other internal and external modes of the chains.

All but two of the nine B_g Tl^+ translational lattice modes expected in Raman scattering are observed (Table IV and Fig. 6). With the instrument used the nine expected A_g bands are masked by the broad Rayleigh band in the $X(ZZ)\bar{X}$ and $X(YY)\bar{X}$ spectra.

When the temperature is raised through the ordered phase the Raman spectra evolve smoothly. As expected for a thermal effect, the width of the bands increases and their wavenumber decrease slightly. The narrowness of the low-frequency bands suggest that the structure is well ordered.

$P2_1/c \leftrightarrow R\bar{3}$ Phase Transition

As the temperature is increased throughout the monoclinic phase, small variations of the wavenumber of the bands are observed and do not remove the splitting found at room temperature. Then in a small range (30 K) of temperature there is a sudden change in the Raman band number.

The evidence for the phase transition is clearly seen in the splitting of the SO_4 internal vibrations Raman bands during the course of the $P2_1/c \leftarrow R\bar{3}$ transition.

The number of Raman bands in the region of the stretching modes of SO_4 moieties agrees with the expected value ($4A_g + 4E_g$) by the factor group analysis (Table V).

TABLE IV

RAMAN FREQUENCIES (cm^{-1}) AT 293 K OF THE MONOCLINIC PHASE OF $Tl_3Cr(SO_4)_3$

Tentative assignment	$X(YY)\bar{X}$, A_g	$X(ZZ)\bar{X}$, A_g	$X(YZ)\bar{X}$, B_g
Stretching	1212 m	1212 w	1218 w
S–O	—	1210 w	1214 w
	1202 m	1202 m	1201 m
	1184 w	1184 w	1184 w
	1176 m	1176 m	
	1122 m	1122 m	1120 w
	1115 m	1115 w	1110 w
	—	1112 m	1095 m
	1096 m	1096 w	1082 w
	1082 w	1082 w	1015 s
	1006 vs	1006 vs	1006 s
			972 vs
			665 w
Asymmetric	602 w		
bending	596 w		595 m
S–O	590 sh	592 w	
	582 m	582 m	582 m
		580 sh	
Stretching	506 s	506 s	506 w
Cr–O	496 s	496 s	496 w
Symmetric	452 w	452 w	
bending	446 m	446 sh	444 w
S–O	442 sh	442 m	424 w
	300 w		
	280 w		
	270 w	270 sh	
	256 s	256 s	258 w
Bending	242 vs	242 vs	242 m
Cr–O	215 w	—	218 w
	205 w	200 w	
		170 sh	168 sh
	160 m		161 s
	140 m	140 sh	
	120 w		124 m
	110 w		110 sh
Tl^+ trans-			61 vs
lation			52 w
			43 m
			40 m
			30 w
			25 w
			20 w

The phase transition is also evident in the temperature-dependent change in splittings of the A_g Cr—O modes near 500 and 250 cm^{-1}.

TABLE V

RAMAN FREQUENCIES (cm^{-1}) AT 370 K OF THE TRIGONAL $R\bar{3}$ PHASE OF $Tl_3Cr(SO_4)_3$

Tentative assignment	$X(YZ)\bar{X}$, A_g	$X(YZ)\bar{X}$, E_g
Stretching	1202 m	1200 s
S–O	1170 m	1170 w[a]
	1112 m	1090 m
	1006 vs	1008 vs
	972 w[a]	974 vs
Asymmetric		664 w
bending	580 w	596 w
S–O		584 w
Stretching	503 s	503 w
Cr–O		
Symmetric	448 w	448 w
bending		424 w
S–O		
Bending	250 vs	250 w
Cr–O		242 w
		228 sh
	150 w	170 sh
	130 w	161 s
		124 m
Tl^+ trans-	63 s	61 w
lation	48 w	47 s
	33 s	29 w

[a] Polarization leakage.

The low-lying A_g and B_g phonons of Tl^+ ions reduce from nine in phase I to three A_g (63, 48, 33 cm^{-1}) and three E_g (61, 47, 29 cm^{-1}) in $R\bar{3}$ phase (Fig. 6). The number of A_g

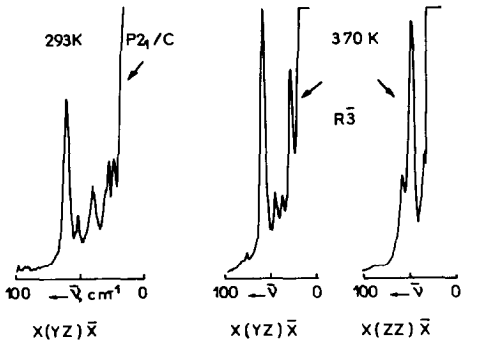

FIG. 6. Polarized low-frequency Raman spectra in $X(ZZ)\bar{X}$ and $X(YZ)\bar{X}$ orientation of $R\bar{3}$ phase of $Tl_3Cr(SO_4)_3$ and $X(YZ)\bar{X}$ orientation of $P2_1/c$ phase. Excitation 514.5 nm.

and E_g translational lattice modes found in the region 0–70 cm^{-1} is in good agreement with $C_{3i}^2 \equiv R\bar{3}$ space group.

The Raman spectra obtained with powder samples exhibit six Raman bands in the range 1250–800 cm^{-1} and three Raman bands are found in the range 0–70 cm^{-1} (Figs. 3, 4) whereas the infrared spectra exhibit four broad bands in the region 1250–800 cm^{-1} and three bands in the range 0–70 cm^{-1} (Fig. 7). The static and dynamic field effects produce A_g, A_u, and E_g, E_u weak splitting not resolved on Raman and IR spectra recorded with powder samples, but they are resolved in the single-crystal spectra (Figs. 5, 6).

In the vicinity of the phase transition temperature, the low-frequency spectra were recorded during the slow increase and subsequent slow decrease of temperature. The phase transition $P2_1/c \rightarrow R\bar{3}$ occurs over a temperature range of 30 to around 340 K. The reversibility of the transformation could not be observed during an experiment due to its slowness, but it is effective after 24 hr at 100 K. The hysteresis temperature range seems very large and characteristic of a first-order transition. It should be noted that a weak pressure effect generates the phase transition $P2_1/c \rightarrow R\bar{3}$ at room temperature.

$R\bar{3} \leftrightarrow R3c$ Phase Transition

As the temperature is increased throughout the $R\bar{3}$ phase, small variations of the wavenumbers of the bands are observed and do not remove the splitting found in the temperature range of the $R\bar{3}$ phase. In a small range of temperature around 450 K, there is a dramatic change in the Raman

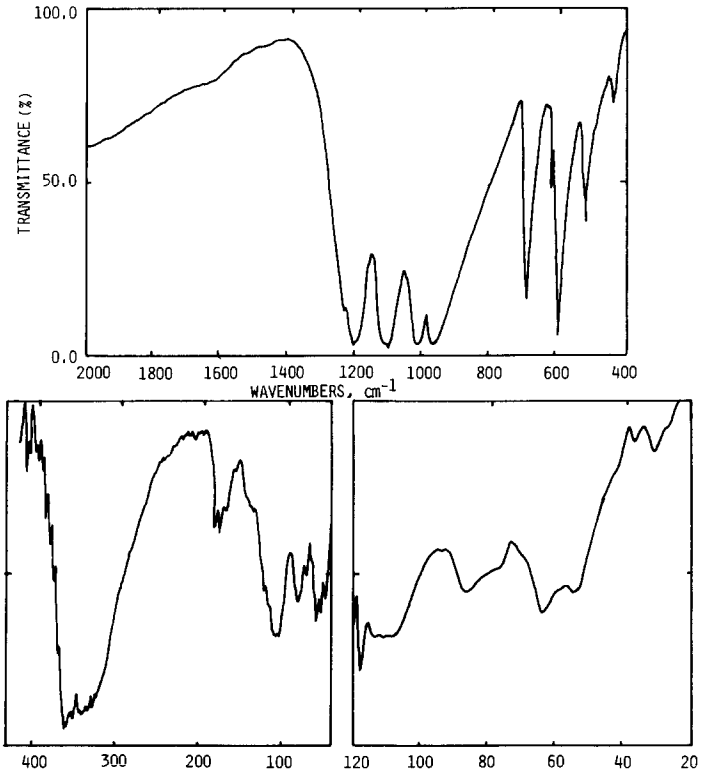

FIG. 7. Infrared spectra of $R\bar{3}$ phase of $Tl_3Cr(SO_4)_3$ powder samples.

spectra. In the vicinity of 450 K, low-frequency spectra were recorded with powder samples (Fig. 4) and with crystal (Fig. 6) during the slow increase of temperature and subsequent slow decrease. The Raman spectrum consisting of well-defined bands extending from 20 to 70 cm^{-1} found just below 450 K changes to a structureless broad band above 450 K with no evidence of "softening" of any mode. The expected lattice vibrations ($3A_1 + 6E$) in the $R3c$ phase are not observed except as a broad shoulder of the Rayleigh band. Although the structure of $Tl_3Cr(SO_4)_3$ has not yet been determined in the $R3c$ phase, we can reasonably assume that $Tl_3Cr(SO_4)_3$ has a structure similar to that of $(NH_4)_3In(SO_4)_3$ in the $R3c$ phase (*2*), because of the great similarities of the Raman spectra and preliminary X-ray study (*7*).

The evidence for the phase transition is clearly seen in the internal vibration Raman bands. The narrow A_g and E_g Raman bands associated with the stretching modes of the SO_4 groups in the $R\bar{3}$ phase evolve to broader A_1 and E bands in the $R3c$ phase. The splittings are not resolved and the expected Raman band number predicted by the factor group analysis is not obtained. In addition, a dramatic temperature effect is observed particularly near 500 cm^{-1} (Fig. 5A), the strong A_g band attributed to Cr–O stretching vibration in CrO_6 octahedra disappears in the $R3c$ phase. The effect of the temperature on the skeletal modes indicates the role of the SO_4 groups in the phase transition which is connected with a dynamic translational disorder of the Tl^+ ions. Indeed, the narrowness of the lattice bands obtained for the $P2_1/c$ and $R\bar{3}$ phases indicate that the structures are well ordered, while on the contrary the extremely broadened lattice bands of the $R3c$ phase indicate a dynamic disorder of the system.

In the low-temperature phase, there are well-defined oxygen polyhedra around Tl^+ ions. The translational lattices modes involving Tl^+ ions frameworks are sensitive to the O . . . Tl bonding scheme ordering. As the temperature increases, different Tl . . . O bonding arrangements may occur and generate dynamic translational disorder. The hysteresis temperature range (40 K) is large and characteristic of a first-order $R\bar{3} \leftrightarrow R3c$ transition.

As the temperature is increased throughout the $R3c$ phase, small variations of the wavenumber and of the width of the bands are observed and are attributed to a normal temperature effect. However, as the temperature increases above 620 K, the shape of the Raman bands evolves smoothly, particularly in the wavenumber ranges associated with the internal modes of SO_4 groups. In the hypothetical prototype cell of $D^6_{3d} \equiv R\bar{3}c$ space group with $Z = 2$ the A_1 and E modes become A_{1g} and E_g Raman active modes (Fig. 8). Unfortunately we were not able to make any deduction from the spectra performed at higher temperature which can confirm the prediction of the group theory.

Apart from the vibrational studies, the transition was also investigated by permitivity measurements which exhibits a well-defined peak at 630 K (*7*).

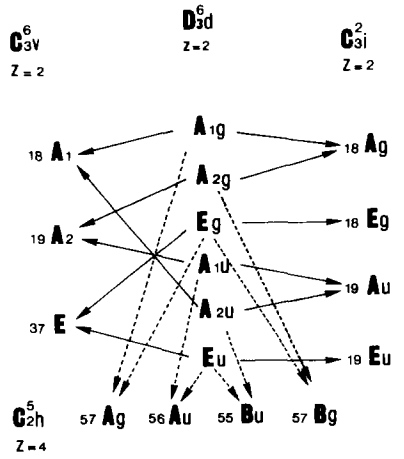

FIG. 8. Correlation table between the C^5_{2h}, C^2_{3i}, C^6_{3v}, and D^6_{3d} symmetry groups exhibited by $Tl_3Cr(SO_4)_3$.

As described previously (*2*) in the phase transition $P2_1/c \leftrightarrow R3c$ which occurs at 400 K in $(NH_4)_3In(SO_4)_3$ the point group $2/m$ is not a subgroup of point group $3m$. Thus the $R3c$ phase cannot be the prototype phase of the monoclinic form $P2_1/c$. Among the several paths which can be imagined to explain the transition sequence, a physically acceptable path has been postulated (*2*) with an intermediate phase with point symmetry $\bar{3}$. If the relationship between the phases of $Tl_3Cr(SO_4)_3$ is considered as follows:

$$2/m \leftrightarrow \bar{3} \leftrightarrow 3m \leftrightarrow \bar{3}m,$$

the space groups $P2_1/c$, $R\bar{3}$, and $R3c$ belong to subgroups of the prototype $R\bar{3}c$ (Fig. 8). The intermediate and prototype phases are well substantiated in the case of $Tl_3Cr(SO_4)_3$. The vibrational studies point out the role played by the SO_4 groups in the phase transitions. The first step is a transition to perfectly symmetrical columns $P2_1/c \rightarrow R\bar{3}$ with a concomitant change of the Tl^+ coordination polyhedra. Then concerning $R\bar{3} \rightarrow R3c$ transformation, a further tilting of all the SO_4 groups, would preserve the relation of symmetry between the different columns. The tilting of the SO_4 groups is connected with a translational disorder of the Tl^+ ions. When the temperature becomes lower than 450 K the interaction forces between O atoms of the SO_4 groups and Tl^+ ions prevail over the thermal agitation.

Acknowledgments

We should like to thank Nicole Le Calvé and Bernadette Pasquier for helpful discussions and Christophe Depecker and Bernard Sombret for infrared spectra.

References

1. B. Jolibois, G. Laplace, F. Abraham, and G. Nowogrocki, *Acta Crystallogr.* **36,** 2717 (1980) and references therein.
2. B. Jolibois, G. Laplace, F. Abraham, and G. Nowogrocki, *J. Solid State Chem.* **40,** 69 (1981).
3. G. Laplace and B. Jolibois, *J. Appl. Crystallogr.* **12,** 615 (1979).
4. M. Delhaye and P. Dhamelincourt, *J. Raman Spectrosc.* **3,** 33 (1975).
5. M. E. Anderson and R. Z. Muggli, *Anal. Chem.* **53,** 1772 (1981).
6. G. Turrell, *J. Raman Spectrosc.* **15,** 103 (1984).
7. F. Abraham, C. Bremard, B. Jolibois, M. Drache, J. Laureyns, and G. Nowogrocki, "Réunion Française de Ferroélectricité," Le Mans, France (1982).
8. A. Goypiron, J. de Villepin, and A. Novak, *Spectrochim. Acta Part A* **31,** 805 (1975).
9. A. Goypiron, J. de Villepin, and A. Novak, *J. Raman Spectrosc.* **9,** 297 (1980).
10. N. Toupry, H. Poulet, and M. Le-Postollec, *J. Raman Spectrosc.* **11,** 81 (1981).
11. R. Mercier, C. Sourisseau, and G. Lucazeau, *J. Raman Spectrosc.* **6,** 195 (1977).
12. G. Lucovsky, R. J. Sladek, and J. W. Allen, *Phys. Rev. B: Condens. Matter* **16,** 4716 (1977).